International Journal of GEOMATE, Oct. 2023, Vol. 25, Issue 110, pp.267-274
ISSN: 2186-2982 (P), 2186-2990 (O), Japan, DOI: https://doi.org/10.21660/2023.110.3996
Geotechnique, Construction Materials and Environment

COMPARISON STUDY OF TORSIONAL STRENGTH OF STEEL FIBER REINFORCED-CONCRETE BEAMS WITH VARIOUS DESIGN CODES

Afif Kusuma Wardana[1] and *Tavio[1]

[1]Department of Civil Engineering, Institut Teknologi Sepuluh Nopember, Surabaya, Indonesia

*Corresponding Author, Received: 26 June. 2023, Revised: 10 Aug. 2023, Accepted: 17 Aug. 2023

ABSTRACT: There has been no calculation of torque capacity using a specific code on SFRC beams. Therefore, this paper describes efforts to compare capacity analysis studies of SFRC beams with ACI Code 318-19 design, CSA A23.3:19, SNiP, Eurocode 2, and modification of ACI Code 318-19. A total of 85 specimens were adopted from 16 previous study groups, and the torsional strength was compared with the proposed equation by modifying and applying it to ACI code 318-19. The proposed formula, by adding the effect of steel fiber, increases the contribution of steel fiber to the longitudinal and transverse reinforcement. After the torsional strength of the proposed formula is obtained, it is compared with the four design codes of torsional strength analysis without the influence of steel fiber to determine the accuracy of the prediction of torsional strength, which is close to the results of experimental testing. From the results presented, each strength design prediction varies significantly in mean ratio, standard deviation, and coefficient of variation. Comparing the five concluded that the design obtained using the modified design code ACI 318-19 and CSA A23.3:19 provides better accuracy. The results of Eurocode 2 provide an average ratio of 1.62, the largest among the others.

Keywords: Codes, Disaster risk reduction, Reinforced concrete beams, Steel fiber, Torsional strength

1. INTRODUCTION

Concrete is an element that is often used in structural components [1]. Concrete has several beneficial properties, including easy-to-obtain raw materials, relatively low prices, easy-to-shape as needed, and low maintenance costs [2,3]. Besides having advantages, concrete has disadvantages, namely its brittle nature, so that the tensile resistance of concrete tends to be weak. Steel reinforcement resists the tensile stresses that arise due to loading in the design of concrete structures [4,5]. Another problem that needs attention is the appearance of cracks in the concrete due to tensile stress [6]. Therefore, additional materials such as steel fiber must overcome these problems [7-9].

The use of steel fibers in concrete mixes became widespread in the 1960s. Combining conventional concrete with the addition of steel fiber, better known as Steel Fiber Reinforcement Concrete (SFRC), can increase the mechanical resistance and increase the absorption of earthquake energy properly [10]. With the addition of steel fiber, it is possible to change the failure mode from brittle failure to ductile failure [11]. SFRC is superior in receiving tensile loads because steel fibers can transmit tensile stress when the concrete is released [12,13]. When the concrete cracks, the concrete matrix and steel fibers become active, which results in friction between the steel fibers embedded in the concrete. Reinforced concrete beams with steel fibers require bending and shear analysis [14,15]. Besides that, torsional behavior is one of the primary considerations needed in accurate beam design [16,17]. Several regulations can be used to design the strength of reinforced concrete beams, such as American Concrete Institute 318-19, Canadian Standards Association A23.3-19, SNiP, and Eurocode 2.

Academics and practitioners do not yet know whether regulations from ACI 318-19 are the most efficient regulations used to plan the torsion of intense reinforced concrete beams to find out which regulations are most suitable for planning reinforced concrete beams with the addition of steel fiber in building structures [18], experimental tests are needed to assess the torsional strength of the SFRC. In this study, the results of the strong torsion testing from several previous studies were compared with the results of analytical calculations using several regulations from various countries, namely ACI 318-19 CSA A23.3-19, SNiP, and Eurocode 2. Review by developing a new formula for strong SFRC torsional by modifying regulation of ACI 318-19 by increasing the stress in the beam due to steel fibers in both the longitudinal and transverse directions. The different aspects of each approach are then compared for testing using experimental tests and analytical calculations to determine the reliability of each torsional potential.

2. RESEARCH SIGNIFICANCE

Equation with reasonable accuracy for determining the torsional strength of SFRC beams still needs to be improved. This research provides a simple equation to predict SFRC torsional strength by modifying the ACI 318-19 equation. Analytical calculations are verified using experimental data that previous researchers have carried out. Academics and practitioners understand that using certain equations gives results with a low level of accuracy, and others give insecure results, causing strength design results to be inefficient.

3. METHODOLOGY

The methodology section is divided into specimen determination, parameters, review of various torsional strength calculation codes (ACI 318-19, CSA A23.3:19, SNiP, Eurocode 2, Modification of ACI 318-19), and modification by adding the influence of steel fibers.

3.1 Parameter and Specimens

Figure 1 illustrates the beam test experiment in which the beam is loaded with a "P" load diagonally until the beam experiences torsion.

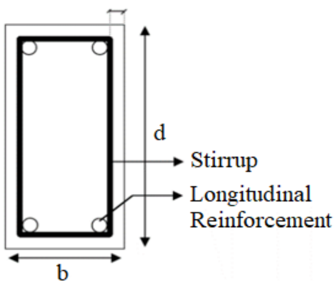

(a)

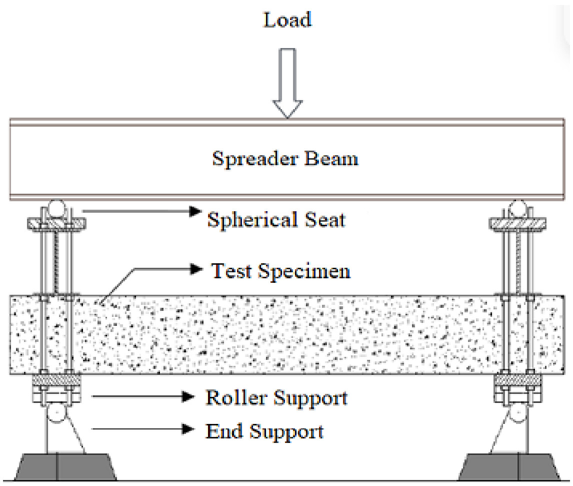

(b)

Fig.1 Illustration of the test setup and loading beam

Table 1 Experimental Beam Data

References	Number of Specimens
Craig et al. [19]	4
Mansur and Lim [20]	4
Narayanan and Palanjian [21]	10
Mansur et.al. [19]	5
Ausi et.al. [22]	2
Kaushik and Sasturkar [22]	3
El Niema [6]	2
Rao and Seshu [24]	12
Chalioris and Karayannis [25]	2
Rao et.al. [26]	12
Okay and Engin [27]	10
Yap et.al. [28]	3
Ju et.al. [29]	2
Premachand and Jayard [30]	3
Amin and Bentz [17]	2
Hassan et.al. [31]	9

In this study, 85 reinforced concrete beams were reinforced with steel fibers with a certain volume ratio and used as an experiment to test the torsional strength. Comparisons were made between the experimental torsional strength divided by the analytical torsional strength, and then the average ratio, standard deviation, and coefficient of variation were obtained. Table 1 shows the number of experimental concrete beams used in this study. Numbers in parentheses indicate journal sources in previous studies beams.

Each parameter of the experimental concrete beams used in this study is shown in Table 2. Out of 85 SFRC beams, the beams with concrete compressive strength of 16-56 MPa were used. In the table, data on the distribution of effective height (*d*), beam width (*b*), concrete quality (f_c), and steel fiber ratio (V_f) were collected and compiled here from previous studies. Figure 2 shows the ratio of the number of specimens to the quality of the concrete in the range of 20 MPa to 60 MPa.

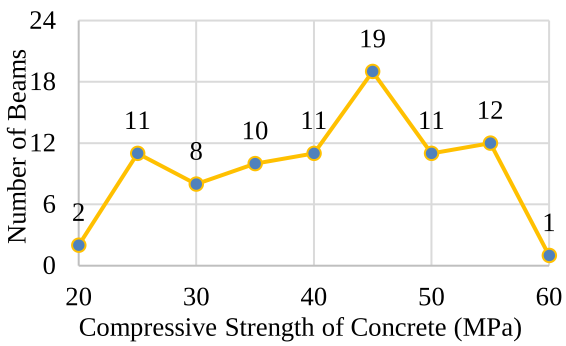

Fig.2 The number of beams on concrete quality

Table 2 Parameter of Experimental Beam Test

b (mm)	d (mm)	f_c (MPa)	V_f (%)
Craig et al. [19]			
152	304.8	29 to 33.8	1 to 2
Mansur and Lim [20]			
100	155	20.5 to 21.6	0.75 to 1.75
Narayanan and Palanjian [21]			
85	178	42.3 to 51.3	0.52 to 1.61
Mansur et al. [19]			
300	300	21.4 to 28	0.5 to 1.5
Ausi et al. [22]			
152	310	40.2	0.5 to 1
Kaushik and Sasturkar [22]			
125	300	24.2 to 26.6	0.5 to 1.5
El Niema [23]			
100	200	35.6 to 38.9	0.6 to 1.2
Rao and Seshu [24]			
100	200	40.1 to 44.1	0.3 to 1.2
Chalioris and Karayannis [25]			
100	200	16.9 to 19	1 to 3
Rao et al. [26]			
100	200	50.1 to 55.5	0.3 to 1.2
Okay and Engin [27]			
150	200	29.5 to 33.4	0.3 to 0.6
Yap et al. [28]			
150	200	35.1 to 36.8	0.5
Ju et al. [29]			
150	250	41.5 to 45.3	1.5 to 2
Premachand and Jayard [30]			
180	180	20.5	0.5 to 1.5
Amin and Bentz [17]			
200	280	42.3	0.38
Hassan et al. [31]			
100 to 200	150 to 300	36.52 to 45.48	0.5 to 1.5

Figure 3 compares the number of specimens to the ratio of steel fiber in the range of 0.3% to 3%, and most fiber is in the range of 0.3% to 1.5%.

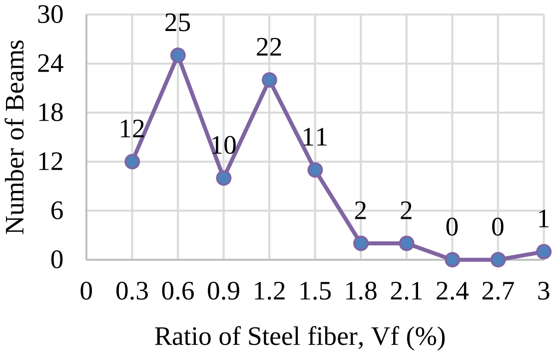

Fig.3 Number of beams against steel fiber

3.2. Review of Various Codes

3.2.1 ACI 318-19

Torsional strength for reinforced concrete beam structures according to ACI 318-19 [18] is calculated using equations (1) and (2), and the smallest value is chosen.

$$T_n = \frac{2A_0 A_t f_{yt}}{s} \cot\theta \tag{1}$$

$$T_n = \frac{2A_0 A_l f_y}{P_h} \tan\theta \tag{2}$$

A_t is the area of one leg of closed transverse reinforcement, A_l the total area of longitudinal reinforcement to withstand torsional stresses, s is the distance between the transverse bars, P_h around the centerline of stirrups, f_{yt} is the yield strength of the transverse bars, f_y the yield of longitudinal reinforcement, and θ is the angle of the diagonal stress in the beam taken from 30 to 60. It is recommended to θ = 45 for non-prestressed beams.

$$A_0 = 0.85\, A_{0h} \tag{3}$$

A_0 it is the area inside the center line of the shear flow zone and A_{0h} the area bounded by the centerline of the stirrup reinforcement [18][32]. The nominal torsional resistance (T_n) must exceed the factor (T_u) and can be calculated by equation (4).

$$T_u = \phi\, T_n \tag{4}$$

ϕ is the torsional reduction factor equal to 0.75.

3.2.2 CSA A23.3:19

The torsional strength of reinforced concrete beams using the CSA code A23.3:19 [33] is calculated using the equation (5). The nominal torsional resistance $\boldsymbol{T_n}$ must exceed the required $\boldsymbol{T_u}$ as shown in equation (6). To obtain $\boldsymbol{T_u}$, $\boldsymbol{T_n}$ multiplied by is a reduction factor for reinforcing steel ϕ_s taken as 0.65.

$$T_n = \frac{A_0 A_t f_{yt}}{s} \cot\theta \tag{5}$$

$$T_u = \phi_s\, T_n \tag{6}$$

The stress angle θ in reinforced concrete beams in equation (7) is related to the longitudinal strain at the mid-depth of the cross-section of the member ε_x as shown in equation (8).

$$\theta = 29° + 7000\, \varepsilon_x \tag{7}$$

The alternative value of $\boldsymbol{\varepsilon_x}$ is allowed to be taken as a larger value than the value with ε_x must remain less than or equal to 0.003.

$$\varepsilon_x \le 0.003 \tag{8}$$

3.2.3 SNiP

The design methods for shear and torsion specified in SNiP are widely adopted in the Western world. The basis of the torsional design model implemented in the SNiP code is the skew-bending theory. After the equations from the skew-bending theory, the torsional strength of concrete components can be estimated using equations (9) and (10) for Mode 1 and Mode 2 failures [23], as follows:

$$T_{n1}=0.5A_{l1}\,f_{yl}h+A_t\,f_{yt}\frac{b^2h}{s(2h+b)} \tag{9}$$

$$T_{n2}=0.5A_{l2}\,f_{yl}h+A_t\,f_{yt}\frac{h^2b}{s(2b+h)} \tag{10}$$

where A_{l1} and A_{l2} are the cross-sectional areas of the reinforcement (bottom face and side face, respectively), h is the cross-sectional height of the beam and b is the cross-sectional width of the beam. To consider the case when the concrete fails before the reinforcement yielding, the calculated torsional strength must be taken as less than the maximum torsional strength (T_{max}), which is determined semi-empirically as follows:

$$T_{max}=0.1\,f_c'\,b^2h \tag{11}$$

The torsional strength is obtained from the minimum value (T_{n1}, T_{n2}, T_{max}).

3.2.4 Eurocode 2

The torsional strength equation in Eurocode 2 is almost identical to ACI 318-19 codes. In addition, it considers the maximum limit for torsional strength corresponding to the failure of concrete crushing [34][35]. Based on Eurocode 2 [36], torsional forces can be estimated as follows:

$$T_n=\frac{A_kA_tf_{yt}}{s}\cot\theta \tag{12}$$

$$T_n=\frac{A_kA_lf_{yl}}{u_k}\tan\theta \tag{13}$$

where $\boldsymbol{A_k}$ is the concrete area enclosed by the effective diameter of the wall thickness, $\boldsymbol{u_k}$ is the perimeter of the midline of the shear flow path, the inclination angle of the strut in EC2 is estimated using the following equation:

$$\theta_{EC}=\cot^{-1}\sqrt{\frac{A_l\,s\,f_{yl}}{A_tu_kf_{yt}}} \tag{14}$$

Moreover, equation (14) is limited to a predetermined angle between $21.8° \leqslant \theta_{EC} \leqslant 45°$.

3.3. Modification of ACI 318-19 Torsion Model for SFRC

ACI design code 318-19 was developed for two potential failure modes. It can be seen from this equation that each consists of two terms, which represent the contribution of the longitudinal and transverse reinforcement to the total torsional resistance of the beam [37-38]. Replace the cross-sectional areas of the steel bars transverse and longitudinal (A_{tst} and A_{lst}) with the total effective cross-sectional areas of the bars, which will take into account both contributions from the steel bars and steel fibers (A_{ttot} and A_{ltot}) [21][24]. Consequently, the following modified ACI 318-19 equation can be obtained for the torsional resistance of SFRC members:

$$T_n=\frac{2A_0A_{ttot}f_{yt}}{s}\cot\theta \tag{15}$$

$$T_n=\frac{2A_0A_{ltot}f_y}{P_h}\tan\theta \tag{16}$$

It is important to consider the zone of effective shear flow thickness. Meanwhile, the equation suggested by [17] to determine the shear flow zone:

$$t_d=0{,}75\frac{A_c}{k} \tag{17}$$

The above equation makes it possible to calculate the effective shear flow thickness zone, which can be calculated based on the properties of the SFRC beam. The effective area carrying shear flow A_e can be calculated using a geometric cross-section with equation 18 [23].

$$A_e=2t_d\,(b+h)-4t_d^2 \tag{18}$$

Where b and h are the cross-sectional width and height of the SFRC beam, respectively. Meanwhile, to determine the number of steel fibers located in the effective zone that contribute to resisting torsional loads by determining the effective ratio (ξ) with equation 19 [23].

$$\xi=\frac{A_e}{A_c} \tag{19}$$

Assuming that the steel fibers are uniformly distributed within the concrete matrix in all directions, the uniformly distributed steel fibers contribute to the transmission of tensile stresses in the transverse and longitudinal directions. The equivalent cross-sectional area that contributes as stress support in the transverse (A_{tf}) and longitudinal (A_{lf}) directions can be calculated as suggested by [23].

$$A_{tf}=\frac{(0{,}5\,\xi\,V_f)\,A_cs}{p} \tag{20}$$

$$A_{lf} = (0{,}5\ \xi V_f)A_c \quad (21)$$

V_f is the ratio of steel fiber contained in the concrete, and s is the spacing of stirrup reinforcement. The equivalent cross-sectional area of the steel fiber calculated by equations (20) and (21) cannot be directly added to the transverse and longitudinal steel reinforcement areas because the characteristics of the steel reinforcement and steel fiber are different. In addition, there is a difference in the stress mechanism between the steel reinforcement and the steel fiber because the steel fiber can withstand the stress due to friction on the surface between the steel fiber and the concrete. The total effective cross-sectional area of reinforcement longitudinal (A_{Itot}) and transverse (A_{Itot}), which is used in equations (22) and (23), can be calculated as follows:

$$A_{Itot}=A_l+A_{lf}\ \frac{\sigma_{max}{}^f}{f_y} \quad (22)$$

$$A_{Itot}=A_t+A_{tf}\ \frac{\sigma_{max}{}^f}{f_{ty}} \quad (23)$$

$$\sigma_{max}{}^f = (0.41)\ \frac{4\ l_b\ \tau_b}{d_f} \quad (24)$$

where $\sigma_{max}{}^f$ is minimum frictional stress between steel fiber, d_f is the diameter of the steel fiber, τ_b is the frictional stress between the bonds and l_b is the length of the fiber embedded in the concrete. The length of fiber embedded in the concrete during the application of loading l_b from $0.5l_f$ to zero due to the increase in crack width and fiber pulling.

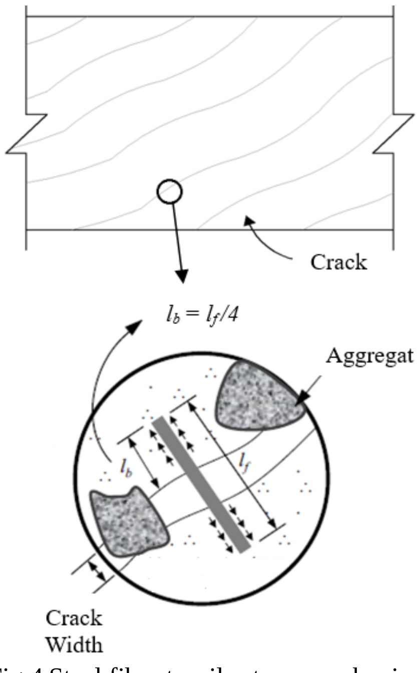

Fig.4 Steel fiber tensile stress mechanism

Therefore, the average value of the fiber embedded in the concrete is $0.25l_f$. Figure 4 shows the mechanism of tensile stress in steel fibers. The steel fiber is randomly distributed in a three-dimensional space with the fiber orientation factor to be taken into account which is equal to 0.41. τ_b can be determined by the equation ($\tau_b = \alpha_f\ \tau_{uf}$) by multiplying the fiber bond factor α_f and the ultimate bond stress (τ_{uf}) between the fiber and the concrete. Figure 5 shows the fiber bonding factor in concrete.

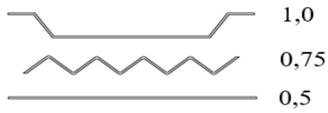

Fig.5 Fiber bonding factor in concrete

τ_{uf} the equation is described according to equation (25).

$$\tau_{uf} \leq 2.5\ f_{ct} \quad (25)$$

where f_{ct} is the concrete tensile stress. It can be calculated using the equation $0.33\sqrt{f_c}$.

4. RESULTS AND DISCUSSION

The ultimate torsional moment values are calculated using the proposed simple and are generated for all SFRC samples in the database and compared with their values obtained experimentally (T_{exp}). Compares the experiment and calculates the torsional strength of the SFRC beam. Statistical parameters that reflect the accuracy of the torsional strength prediction comparison are presented in Table 3.

Table 3 Torsional strength summary for all torsional designs

No.	Code	Statistical Result V_{exp}/V_{calc} Avg	SD	COV
1.	ACI 318-19	1.43	0.91	63.31
2.	CSA A.23.3:19)	1.23	0.89	72.55
3.	SNiP	1.36	0.66	48.79
4.	Eurocode 2	1.62	0.88	54.25
5.	ACI 318-19 Modification	1.02	0.40	39.35

For most cases, the ratio of the analytic ultimate torsional moment to the value calculated by some codes is between 1.0 and 1.7. Calculations referring to Eurocode 2 show that the average ratio of the test force to the calculation is 1.62 with a COV value of

54.25%, more spread out than the predictions of other torsion strength designs. Eurocode 2 calculations provide a fairly conservative prediction and are still on the safe side. The underlying reason for this occurrence is partly attributed to the equation of cross-factor effect size equations.

Unlike Eurocode 2, torque strength prediction is provided by ACI 318-19, CSA. A.23.3:19 and SNiP are shown more accurately. The ratio of the test average to the calculated torsional strength for ACI 318-19, CSA. A.23.3:19 and SNiP 1.43, 1.23, and 1.35, with COV of 63.31%, 72.55%, and 48.79%, respectively. The results show that SNiP has accuracy comparable to ACI 318-19; different from the others, the calculation of CSA A.23.3:19 has the highest level of accuracy.

The mean ratio is 1.02 with a standard deviation of 0.40 and a COV of 39.35, which indicates the accuracy of the proposed model based on a modification of ACI code 318-19. The modified model is on the conservative side, indicating that the model is applicable in practice for design purposes and can account for the contribution of steel fiber to torsional strength.

Overall, each method is comparable in performance, generally works well, and tends to yield conservative predictions, particularly for beams that fail by yielding transverse and longitudinal reinforcement. Figure 6 to Figure 10 shows a comparison of the calculation of the torsional strength to the experimental one, showing that the overall analysis tends to be conservative.

The purpose of the modification is to simplify the calculation of the torque capacity by modifying the analysis from ACI code 318-19 by considering the influence of steel fiber from the analytical approach. The torsion beam strength calculated by the modified ACI equation from code 318-19 has increased. This increase is more significant in the steel fiber factor and experiences an approach to the experimental value.

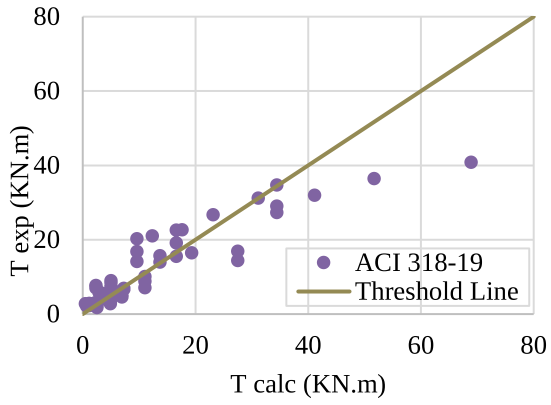

Fig.6 Experimental versus analytic torsional strength (ACI 318-19)

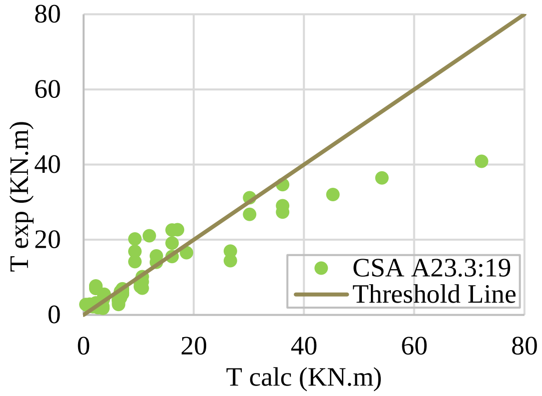

Fig.7 Experimental versus analytic torsional strength (CSA A.23.3:19)

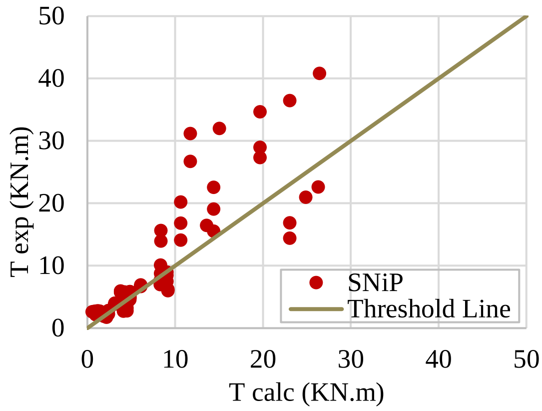

Fig.8 Experimental versus analytic torsional strength (SNiP)

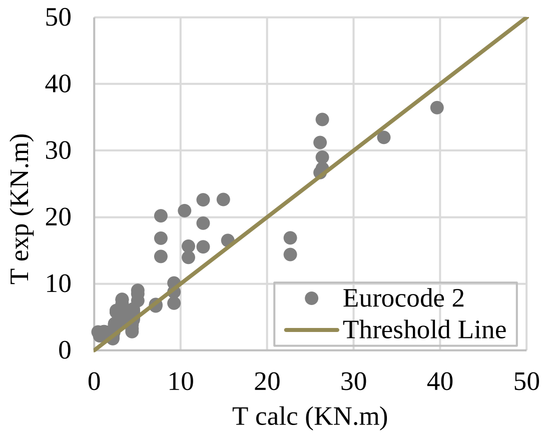

Fig. 9 Experimental versus analytic torsional strength (Eurocode 2)

5. CONCLUSIONS

Based on the calculation of the predictive analysis of the torsional strength of reinforced beams with the addition of steel fiber, emphasis has been placed on evaluating the accuracy of the five torsion design equations of code of practice against 85 experimental assays selected from the SFRC beam of six different research groups. Results of analytical studies in the form of the ratio of calculations to the strength of the experimental test. Based on the research that has been presented, several conclusions can be drawn:

1. The modified ACI 318-19 provides a more accurate prediction than ACI 318-19. The effect of adding the steel fiber factor in the equation shows a more relevant prediction.
2. The average of the calculated to-test strength ratios of all the torsional strength design equations is shown to give conservative results above one. However, it should be noted that some of the test data predicted by Eurocode 2 are too high.
3. Standard ACI 318-19 modification gives the best results compared to the five calculation methods.

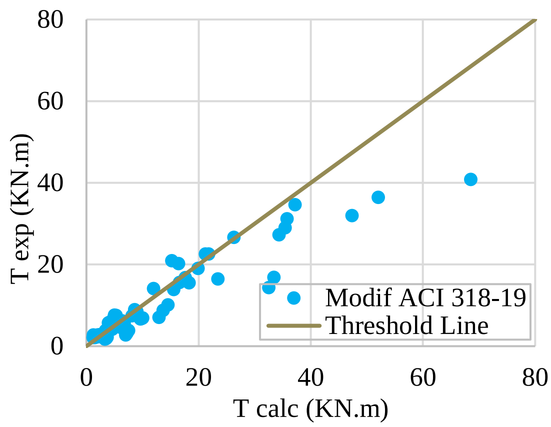

Fig. 10 Experimental versus analytic torsional strength (ACI 318-19 Modification)

6. ACKNOWLEDGMENTS

The authors gratefully acknowledge financial support from the Institut Teknologi Sepuluh Nopember for this work, under project scheme of the Publication Writing and IPR Incentive Program (PPHKI) 2023.

7. REFERENCES

[1] Christianto D., and Makarim C.A., Influence of Longitudinal Reinforcement Ratio on Shear Capacity of No Coarse-Aggregate Concrete, Int. J. GEOMATE, Vol. 21, No. 86, 2021, pp. 122–130.

[2] Ahmad H.H., and Tavio, Experimental Study of Cold-Bonded Artificial Lightweight Aggregate Concrete, AIP Conf. Proc., Vol. 1977, No. 030011, 2018, pp. 1–8.

[3] Sandjaya A., and Christianto D., Experimental Study of Mortar Compressive Strength with Anadara Granosa Powder as a Substitute for Partial Use of Cement, IOP Conf. Ser.: Mater. Sci. Eng., Vol. 650, No. 012037, 2019, pp. 1–6.

[4] Anggraini R., Raka IG.P., and Agustiar, Stress-Strain Relationship of High-Strength Steel (HSS) Reinforcing Bars, AIP Conf. Proc., Vol. 1964, No. 020025, 2018, pp. 1–8.

[5] Tavio, Anggraini R., Raka IG.P., and Agustiar, Tensile Strength/Yield Strength (TS/YS) Ratios of High-Strength Steel (HSS) Reinforcing Bars, AIP Conf. Proc., Vol. 1964, No. 020036, 2018, pp. 1–8.

[6] Bu J., Chen X., Hu L., Yang H., and Liu S., Experimental Study on Crack Propagation of Concrete under Various Loading Rates with Digital Image Correlation Method," Int. J. Concr. Struct. Mater., Vol. 14, No. 25, 2020, pp. 1–25.

[7] Wulandari M., and Sofianto M.F., Split Tensile and Flexural Strength of Concrete with Artificial Lightweight Aggregate (ALWA) and Steel-Fiber, IOP J. Phys.: Conf. Ser., Vol. 1569, No. 042025, 2020, pp. 1–7.

[8] Sabariman B., Soehardjono A., Wisnumurti, and Wibowo A., Stress-Strain Model for Confined Fiber-Reinforced Concrete under Axial Compression, Arch. of Civ. Eng., Vol. 66, No. 2, 2020, pp. 119–133.

[9] Sabariman B., Soehardjono A., Wisnumurti, and Wibowo A., Stress-Strain Behavior of Steel Fiber-Reinforced Concrete Cylinders Spirally Confined with Steel Bars, Adv. in Civ. Eng., Vol. 2018, No. 6940532, 2018, pp. 1–8.

[10] Honestyo A., and Ardhyananta H., Axial Compressive Behavior of Bubble-Size Plastic Straw Waste FRP-Confined Circular Concrete, Int. J. on Eng. Appl., Vol. 11, No. 2, 2023, pp. 73–80.

[11] Amin A., Foster S.J., and Kaufmann W., Instantaneous Deflection Calculation for Steel Fibre Reinforced Concrete One-Way Members, Eng. Struct., Vol. 131, 2017, pp. 438–445.

[12] Rizqyani N., and Tavio, Proposed Formula and Comparison of Shear Strengths of Reinforced Concrete Beams under Various Codes, Int. J. GEOMATE, Vol. 23, No. 99, 2022, pp. 9–16.

[13] Tavio, and Rizqyani N., Proposed Modified Formula for Predicting Shear Strength of Reinforced Concrete Beams Based on Eurocode Approach, Int. J. on Eng. Appl., Vol. 11, No. 1, 2023, pp. 64–72.

[14] Christianto D., and Kurniadi D., Effect of Steel Fiber on Shear Strength of Reactive Powder Concrete, IOP Conf. Ser. Mater. Sci. Eng., Vol. 508, No. 1, 2019.

[15] Christianto D., Makarim C.A., and Liucius Y. U., Size Effect on Shear Stress of Concrete Beam without Coarse Aggregate, IOP J. Phys. Conf. Ser., Vol. 1477, No. 5, 2020.

[16] Tavio, Interactive Mechanical Model for Shear Strength of Deep Beams, J. Struct. Eng. Am. Soc. Civ. Eng., Vol. 132, No. 5, 2006, pp. 826–827.

[17] Amin A., and Bentz E.C., Strength of Steel Fiber Reinforced Concrete Beams in Pure Torsion, Struct. Concr., Vol. 19, No. 3, 2018, pp. 684–694.

[18] ACI Committee 318, Building Code Requirements for Structural Concrete, American Concrete Institute, 2019, 624 pp.

[19] Deifalla A.F., Zapris A.G., and Chalioris C.E., Multivariable Regression Strength Model for Steel Fiber-Reinforced Concrete Beams under Torsion, Materials (Basel), Vol. 14, No. 14, 2021, pp. 1–24.

[20] Mansur M.A., and Lim T.Y., Torsional Behaviour of Reinforced Fibre Concrete Beams, Int. J. of Cem. Comp. and Lghtwght Conc., Vol. 7, No. 4, 1985, pp. 261–267.

[21] Narayanan R., and Kareem A.S., Torsion in Beams Reinforced with Bars and Fibers, J. Struct. Eng., Vol. 112, No. 1, 1986, pp. 53–66.

[22] Ju H., Lee D.H., Hwang J.H., Kang J.W., Kim K.S., and Oh Y.H., Torsional Behavior Model of Steel-Fiber-Reinforced Concrete Members Modifying Fixed-Angle Softened-Truss Model, Compos. Part B Eng., Vol. 45, No. 1, 2013, pp. 215–231.

[23] Ju H., Lee D.H., and Kim K.S., Minimum Torsional Reinforcement Ratio for Reinforced Concrete Members with Steel Fibers," Compos. Struct., Vol. 207, 2019, pp. 460–470.

[24] Rao T.D.G., and Seshu D.R., Analytical Model for Torsional Response of Steel Fiber Reinforced Concrete Members under Pure Torsion, Cem. Concr. Compos., Vol. 27, No. 4, 2005, pp. 493–501.

[25] Chalioris C.E., and Karayannis C.G., Effectiveness of the Use of Steel Fibres on the Torsional Behaviour of Flanged Concrete Beams, Cem. Concr. Compos., Vol. 31, No. 5, 2009, pp. 331–341.

[26] Rao T.D.G., Seshu D.R., and Warnitchai, Effect of Steel Fibers on the Behavior of Over-Reinforced Beams Subjected to Pure Torsion, Civ. Eng., Vol. 12, No. 1, 2010, pp. 44–51.

[27] Okay F., and Engin S., Torsional Behavior of Steel Fiber-Reinforced Concrete Beams, Constr. Build. Mater., Vol. 28, No. 1, 2012, pp. 269–275.

[28] Yap S.P., Khaw K.R., Alengaram U.J., and Jumaat M.Z., Effect of Fibre Aspect Ratio on the Torsional Behaviour of Steel Fibre-Reinforced Normal-Weight Concrete and Lightweight Concrete, Eng. Struct., Vol. 101, 2015, pp. 24–33.

[29] Ju H., Kim K.S., Lee D.H., Hwang J.H., Choi S.H., and Oh Y.H., Torsional Responses of Steel Fiber-Reinforced Concrete Members, Compos. Struct., Vol. 129, 2015, pp. 143–156.

[30] Premachand J.P., Enhancement of Torsional Strength of Reinforced Concrete by Application of Steel Fibres, Int. J. Innov. Res. Sci. Technol., Vol. 2, No. 11, 2016, pp. 590–595.

[31] Hassan R.F., Al-Salim N.H., Mohammed N.S., and Hussein H.H., Experimental Study and Theoretical Prediction on Torsional Strength with Different Steel Fiber Reinforced Concrete and Cross-Section Areas," Eng. Struct., Vol. 251, No. PA, 2022, pp. 113559.

[32] Christianto D., Makarim C.A., and Jusuf A.H., A Proposed Formula for Predicting Size Effect on Shear Strength of Concrete Beams without Coarse Aggregate, Int. J. on Eng. Appl., Vol. 10, No. 3, 2022, pp. 220–226.

[33] Kuan A., Bruun E.P.G., Bentz E.C., and Collins M.P., Alternative Design Procedures for Torsion in ACI 318-19: A Comparative Study, Am. Concr. Institute, ACI Spec. Publ., vol. SP-344, 2020, pp. 64–91.

[34] Ju H., Lee D.H., Kim J.R., and Kim K.S., Maximum Torsional Reinforcement Ratio of Reinforced Concrete Beams, Structures, Vol. 23, No. 7, 2020, pp. 481–493.

[35] Christianto D., Makarim C.A., and Pratama I.D., Modified EC2's Shear Strength Equation for No Coarse Aggregate RC Beams, Int. J. Adv. Sci. Eng. Inf. Technol., Vol. 12, No. 6, 2022, pp. 2211–2216.

[36] Raut L.L., and Kulkarni D., Torsional Strengthening of Under Reinforced Concrete Beams using Crimped Steel Fiber, Int. J. Res. Eng. Technol., Vol. 3, No. 6, 2014, pp. 466–471.

[37] Teng S., and Tavio, Effective Torsional Rigidity of Reinforced Concrete Members, ACI Struct. J., Vol. 101, No. 2, 2004, pp. 252–260.

[38] Honestyo A., and Ardhyananta H., Tensile Properties of Woven Plastic Straw Waste Fiber-Reinforced Polymer Composites, Int. J. on Eng. Appl., Vol. 11, No. 1, 2023, pp. 11–17.